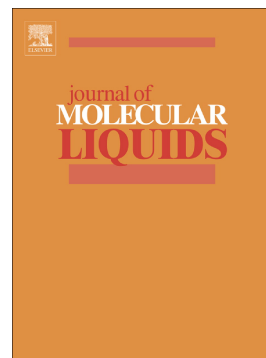


Synthesis, assessment and corrosion protection investigations of some novel peptidomimetic cationic surfactants: Empirical and theoretical insights

Wessam S. Abdrabo, Bahaa Elgendy, Kamal A. Soliman, Hany M. Abd El-Lateef, Ahmed H. Tantawy



PII: S0167-7322(20)32352-7

DOI: <https://doi.org/10.1016/j.molliq.2020.113672>

Reference: MOLLIQ 113672

To appear in: *Journal of Molecular Liquids*

Please cite this article as: W.S. Abdrabo, B. Elgendy, K.A. Soliman, et al., Synthesis, assessment and corrosion protection investigations of some novel peptidomimetic cationic surfactants: Empirical and theoretical insights, *Journal of Molecular Liquids* (2018), <https://doi.org/10.1016/j.molliq.2020.113672>

This is a PDF file of an article that has undergone enhancements after acceptance, such as the addition of a cover page and metadata, and formatting for readability, but it is not yet the definitive version of record. This version will undergo additional copyediting, typesetting and review before it is published in its final form, but we are providing this version to give early visibility of the article. Please note that, during the production process, errors may be discovered which could affect the content, and all legal disclaimers that apply to the journal pertain.

Synthesis, assessment and corrosion protection investigations of some novel peptidomimetic cationic surfactants: empirical and theoretical insights

Wessam S. Abdrabo^a, Bahaa Elgendy^{a,c,d,*}, Kamal A. Soliman^a, Hany M. Abd El-Lateef^{b, e,*},

Ahmed H. Tantawy^{a,f,*}

^a*Department of Chemistry, Faculty of science, Benha University, Benha-13518, Egypt*

^b*Department of Chemistry, College of Science, King Faisal University, P.O. Box 380 Al Hofuf 31982 Al-Ahsa, Saudi Arabia*

^c*Department of Pharmaceutical and Administrative Sciences, St. Louis College of Pharmacy, St. Louis, MO 63110, USA*

^d*Center for Clinical Pharmacology, Washington University School of Medicine and St. Louis College of Pharmacy, St. Louis, MO 63110, USA*

^e*Chemistry Department, Faculty of Science, Sohag University, Sohag-82534, Egypt*

^f*Department of Chemistry, College of Science, Huazhong Agricultural University, Wuhan, 430070, China*

***Corresponding authors:** ahmed.tantawy@mail.hzau.edu.cn (Ahmed H. Tantawy),

hmahmed@kfu.edu.sa (H. M. Abd El-Lateef), bahaa.elgendy@stlcop.edu (Bahaa

Elgendy).

Abstract

Three novel peptidomimetic cationic surfactants were synthesized in good yields. The chemical configurations of these surfactants were clarified using ^1H , ^{13}C NMR and FT-IR spectroscopy. The inhibition capacity and adsorption performance of these compounds on C-steel were studied by electrochemical techniques (Electrochemical impedance spectroscopy (EIS) and Potentiodynamic polarization (PDP) methods). The prepared compounds demonstrated outstanding protection power for the erosion of C-steel in 0.5 M HCl at 323 K. The PDP studies demonstrated that the novel surfactants behaved as mixed-type additives. The protection capacity rises with an increasing surfactant dose, with values ranging from 93.10 to 98.25% at 100 ppm. The adsorption of additives on the electrode interface follows the Langmuir model and contains chemisorption modes. The **Monte Carlo** (MD) simulations and density functional theory (DFT) calculations support the experimental findings and provide insight into the understanding of the adsorption features and protection performance mechanisms of the examined surfactants.

Keywords: Peptidomimetics; Surfactants; Acid inhibition; MD simulations; DFT

1. Introduction

Metallic corrosion is a major problem for the application of engineering materials in various environments.[1,2]. As a result, there are ongoing efforts to develop protective tools that can effectively protect the materials from corrosion.[3] There is no one solution to be used against the corrosion of all metals across different aggressive media. Surfactants are used as corrosion inhibitors to slow down the deterioration of metals [4–6].

Cationic surfactants are widely known for their corrosion inhibition activity,[7–13] especially quaternary ammonium compounds, which are important corrosion inhibitors in acidic media [7–9]. The anti-corrosive effect of adding halide[14] or increasing the alkyl chain length have been extensively studied [15]. Cationic surfactants are amphiphilic compounds with self-assembling properties and can dissociate in water to form surface-active cations. Because of these cationic amphiphilic properties, cationic surfactants have high application potential in many fields [16]. For example, they can be used as follows: in drug delivery as drug and gene nano-carriers, [17] stabilizers of nanoparticles and nano-carriers,[18–20] antimicrobial and bioimaging agents, [21,22] supramolecular catalysts;[23,24] additionally, they can be applied for the removal of drugs [25] and organic pollutant [26] from aqueous media and in thermal energy storage applications through enhancing the heat storage capacity of metal hydroxide[27]. Quaternary ammonium compounds have a high affinity for biopolyanions, such as DNA [28–30].

Amino acids and peptide-based surfactants or peptidomimetic surfactant have many promising applications that have been explored in various ways, especially for their antimicrobial activities[31–33] and self-assembly nano-structure formation [34]. Toxicity, biodegradability, and bioaccumulation are now highly important criteria for deciding to apply any surfactant.[35] The combination of quaternary ammonium compounds with peptidomimetic moiety should produce a promising class of peptidomimetic surfactants that

combine the anti-corrosive activity of quaternary ammonium compounds with the antimicrobial and antifungal activities of the peptidomimetic compounds, while also having quick biodegradation properties.[16]

It is worth noting that the alkyl chain length of cationic surfactants may affect the interactions between the molecules and metals, resulting in the effect of corrosion inhibition.[11,36,37]. Therefore, three peptidomimetic compounds with different alkyl chain lengths were designed and employed for C-steel corrosion protection for the first time.

The molecular structures of the synthetic peptidomimetic surfactants are presented in Fig. 1. The corrosion inhibition performance of the synthetic molecules was studied by taking electrochemical measurements and performing a surface tension analysis. DFT calculations, MD simulations and adsorption isotherms were utilized to further study the corrosion inhibition mechanism. In this report, we studied the anticorrosion properties of newly developed peptidomimetic cationic surfactants with different alkyl chains.

2. Experimental Technique

2.1 Materials

Benzoyl benzotriazole, acetylacetone (98.0%), *N,N*-dimethylpropane-1,3-diamine (99.9%) and 2-chloroacetylchloride (98.0%) were obtained from Aldrich company. Benzoic acid, 1-decanol, 1-tetradecanol and 1-hexadecanol were purchased from Acros Organics (Belgium). Diethyl ether (99%), triethylamine (97%), K_2CO_3 (anhydrous), benzene (98%), and ethanol (99%) were obtained from El Nasr Company, Egypt.

The structure compositions of the C-steel used for the erosion experiments are (in weight percent): Mn (0.72%), C (0.18%), Ni (0.02%), S (0.05%), Cr (0.01%), and rest iron.

The aggressive medium of hydrochloric acid (0.5 M) was designed by mitigating the 37% HCl (analytical grade) with bidistilled H_2O . Different concentrations (10–100 ppm) of

the synthesized surfactants were similarly prepared in double-distilled H₂O and utilized as additives for the C-steel corrosion in 0.5 M HCl.

2.2. Instruments

The FTIR analysis was performed at Benha University, Egypt via a thermo Nicolet iS10 FTIR spectrophotometer using potassium bromide. The NMR spectra were recorded on a Bruker NMR spectrometer operating at 400 MHz for ¹H NMR and 100 MHz for ¹³C NMR. The chemical shifts were referenced to the solvent peak.

2.3. Surfactants Synthesis

Synthesis of benzoyl benzotriazole

SOCl₂ (0.15 mL, 4.2 mmol) was added with stirring at 25°C to a benzotriazole solution (2.0 g, 16.8 mmol) in dichloromethane (DCM) (15.0 mL). After 0.5 h, a solution of benzoic acid (0.512 g, 4.2 mmol) in DCM (10 mL) was added to one portion and stirred for 120 min. The white precipitate was filtered off, followed by washing with DCM (20 mL), and the collective organic solution was washed with aq. NaOH (2N) (3.0 × 15.0 mL) and desiccated over Na₂SO₄; then, the DCM was evaporated under a vacuum to obtain benzoyl benzotriazole (0.81 g, 86.4%).

Synthesis of hippuric acid

To a solution of benzoyl benzotriazole (0.447 g, 2.0 mmol) in acetonitrile (6 mL), glycine (0.15 g, 2 mmol) in acetonitrile/water (6/4 mL) and triethylamine (0.102 g, 1 mmol) were added under stirring at 25°C. After the stirring the, mixture was allowed to react for 2 h; then, it was dilute by water (10 mL) and extracted by DCM (3 × 15 mL) to remove the excess of benzotriazole. The water was concentrated to obtain the crystalline hippuric acid (0.275 g, 77%). The reaction was repeated with the same conditions on (1.24 g, 5.0 mmol) of benzoyl benzotriazole, and the yield was 74%.

Synthesis of 4-(4-methoxybenzylidene)-2-phenyloxazol-5(4H)-one (3)[38].

A mixture of sodium acetate (0.82 g, 10 mmol), (0.9 g, 5 mmol) hippuric acid and acetic anhydride (5 mL) was stirred at 25°C for 30 min. 4-Methoxy benzaldehyde (0.61 mL, 5 mmol) was added to the reaction solution and stirring of the solution continued for an additional 6 h. The reaction was quenched by frozen H₂O and washed by sodium carbonate. The precipitate was collected and recrystallized from ethanol to obtain yellow fluffy crystals of compound **3** (1.1 g, 78.7%).

Synthesis (Z)-N-(3-((3-(dimethylamino)propyl)amino)-1-(4-methoxyphenyl)-3-oxoprop-1-en-2-yl)benzamide (4)

Compound **3** (0.56 g, 2 mmol) was dissolved in 5 mL DCM; then *N,N*-dimethyl propyl amine (0.38 mL, 3 mmol) was added. The reaction mix was stirred for 0.5 h. at 25°C, and then the solvent was separated under vacuum to give the desired product as white crystals (0.57 g, 75%); mp 139-141 °C. IR(KBr) ν_{\max} : 3247, 3070, 2973, 2942, 2855, 2763, 1655, 1640, 1606, 1507, 1478, 1278, 1254. ¹H NMR (400 MHz, DMSO-*d*₆) δ 9.82 (s, 1 H, -NH-), 8.15 (t, J = 5.5 Hz, 1 H, -NH-), 8.04 (dt, J = 7.0, 1.4 Hz, 2 H, aromatic CH), 7.65 – 7.47 (m, 5 H aromatic CH), 7.26 (s, 1 H, aromatic CH), 6.95 – 6.86 (m, 2 H, aromatic CH), 3.73 (s, 3 H, OCH₃), 3.19 (q, J = 6.5 Hz, 2 H, NH-CH₂-), 2.22 (t, J = 6.8 Hz, 2 H, CH₂-N), 2.01 (s, 6 H, N(CH₃)₂), 1.57 (p, J = 6.8 Hz, 2 H, -CH₂-). ¹³C-NMR (DMSO-*d*₆, 101 MHz) δ 213.85, 208.54, 201.77, 183.56, 167.49, 165.46, 164.64, 159.39, 133.63, 131.35, 130.73, 129.07, 128.05, 127.82, 127.60, 126.61, 113.81, 57.27, 55.00, 44.86, 38.19, 26.35.

Synthesis of 2-chloroacetate derivatives: It was prepared according to our previous work [39].

Synthesis of (Z)-3-(2-benzamido-3-(4-methoxyphenyl)acrylamido)-N-(2-(hexadecyloxy)-2-oxoethyl)-N,N-dimethylpropan-1-aminium (5a-c)

A solution of 2-chloroacetate derivatives (1.51 mmol) in 10.0 mL of ethyl ethanoate was prepared and mixed with a solution of **4** (0.38 g, 1 mmol) in 20 mL of ethyl acetate with

continuous stirring. The reaction system was taken to reflux at 70°C for 48 h. The product precipitated upon allowing the reaction solution to cool. The obtained yields were washed via diethyl ether to separate the undesired reactants. By column chromatography (CH₂Cl₂: MeOH, 10:1.5), the product was purified to generate the target cationic surfactants (**5a-c**) with varying yields and colors.

(Z)-3-(2-Benzamido-3-(4-methoxyphenyl)acrylamido)-N-(2-(hexadecyloxy)-2-oxoethyl)-N,N-dimethylpropan-1-aminium (WA-1, 5a). Yield: 55%, pale yellow crystals; mp 148-150 °C. IR(KBr) ν_{\max} : 3243, 3072, 2972, 2947, 2852-2767, 1758, 1644, 1606, 1513, 1477, 1283, 1254. ¹H NMR (400 MHz, DMSO-*d*₆) δ 9.93 (s, 1 H, NH), 8.14 (s, 1 H, NH), 7.53 (d, *J* = 7.7 Hz, 4 H, aromatic CH), 7.25 (s, 1 H, aromatic CH), 7.16 (s, 1 H, aromatic CH), 6.92 (t, *J* = 8.8 Hz, 4 H, aromatic CH), 4.45 (s, 2 H, CH₂), 4.17 (d, *J* = 7.8 Hz, 2 H, CH₂), 3.75 (s, 3 H, OCH₃), 3.20 (s, 6 H, N(CH₃)₂), 2.14 (d, *J* = 8.7 Hz, 2 H, CH₂), 1.96 (s, 2 H, CH₂), 1.63 (t, *J* = 7.6 Hz, 4 H CH₂-CH₂), 1.25 (s, 26 H, (CH₂)₁₃), 0.87 (m, 3 H, CH₃). ¹³C NMR (DMSO-*d*₆, 100 MHz) δ 166.19, 165.45, 165.19, 160.09, 132.04, 131.48, 129.70, 128.90, 128.73, 128.51, 128.40, 128.31, 114.51, 66.37, 63.81, 61.47, 57.55, 55.70, 51.63, 45.14, 34.25, 31.70, 29.44, 29.08, 28.30, 26.70, 25.67, 23.14, 22.48, 14.31.

(Z)-3-(2-Benzamido-3-(4-methoxyphenyl)acrylamido)-N,N-dimethyl-N-(2-oxo-2-(tetradecyloxy) ethyl)propan-1-aminium (WA-2, 5b). Yield: 61%, pale yellow crystals; mp 115-118 °C.

(Z)-3-(2-Benzamido-3-(4-methoxyphenyl)acrylamido)-N-(2-(decyloxy)-2-oxoethyl)-N,N-dimethylpropan-1-aminium (WA-3, 5c). Yield: 61%, pale yellow semisolid at room temp. IR(KBr) ν_{\max} : 3241-3220, 3026, 2922, 2852, 1754, 1648, 1606, 1514, 1477, 1283, 1254. IR(KBr) ν_{\max} : 3243, 3072, 2972, 2947, 2852-2767, 1758, 1644, 1606, 1513, 1477, 1283, 1254. ¹H NMR (DMSO-*d*₆, 400 MHz) δ 10.02 (s, 1 H, NH), 8.20 (s, 1 H, NH), 8.09 (s, 2 H, aromatic CH), 7.56 (d, *J* = 22.0 Hz, 5 H, aromatic CH), 7.22 (s, 1 H, aromatic CH), 6.93

(s, 1 H, **aromatic CH**), 6.91 (s, 1 H, **aromatic CH**), 4.52 (s, 2 H, **CH₂**), 4.19 (s, 2 H, **CH₂**), 3.76 (s, 3 H, **OCH₃**), 3.63 (s, 2 H, **CH₂**), 3.27 (s, 6 H, **N(CH₃)₂**), 1.97 (s, 2 H, **CH₂**), 1.63 (s, 2 H, **CH₂**), 1.26 (s, 16 H, **(CH₂)₈**), 0.87 (s, 3 H, **-CH₃**). ¹³C NMR (DMSO-*d*₆, 100 MHz) δ 166.45, 166.17, 165.26, 160.09, 134.24, 132.05, 131.50, 129.21, 128.69, 128.58, 128.46, 127.24, 114.48, 66.33, 63.73, 61.43, 55.70, 51.53, 36.44, 31.71, 29.39, 29.08, 28.31, 25.67, 23.07, 22.48, 14.31.

2.4. Corrosion inhibition measurements

All corrosion tests were conducted on the VersaSTAT4 potentiostat/galvanostat connected with an electrochemical cell system containing 3-electrodes including working (C-steel), reference (saturated calomel electrode; SCE) and counter electrodes (Pt wire). Approximately 45 min was permitted for the corrosion system to reach the open circuit potential (E_{ocp}) after the exposure of the carbon steel prior to each electrochemical experiment.

Electrochemical impedance spectroscopy (EIS) was implemented using a VersaSTAT4 potentiostat/galvanostat, controlled by means of a frequency response analyzer (FRA). The frequency extended from 100×10^3 Hz to 0.5 Hz with an ac voltage capacity of 0.010 V. The potentiodynamic polarization (PDP) plots were achieved by sweeping the potential up to ± 250 mV vs. E_{corr} at a sweep rate of 0.2 mV/s. All the corrosion measurements were performed under unstirred aerated environments at 50 °C. All the electrochemical tests were repeated three times to ensure the accuracy of the experimental data.

2.5. Surface activities

The surface tension (γ) values of the obtained cationic surfactants at 298 K were investigated via a Tensiometer-K6 processor (Krüss Company, Germany). For calibration, the ring was cleaned between the measurement runs with distilled water and acetone. Before the measurements were taken, all the aqueous solutions of the obtained cationic surfactants

continued to stand 1-2 h. Each concentration of the synthesized compounds was measured three times at the same temperature, and the average value was recorded and taken. From the γ values, the surface activity parameters will be calculated.

2.6. Electrical conductivity

The electrical conductivity measurements of the synthesized compounds were performed via a model Type AD3000 digital conductivity/temperature meter, with EC/TDS at a certain temperature (298 K). All the measurement values were repeated three times for each surfactant solution and the data were recorded.

2.7. Theoretical Studies

In this work, the geometry of the two inhibitor molecules (**WA-1** and **WA-2**) were fully optimized via density functional theory (DFT) hybrid functional B3LYP[40] in the gas and liquid phases. The polarizable conductor calculation model (CPCM) was used to simulate water as a solvent [41]. The calculations were based on the 6-311G (d,p) basis set. Quantum descriptors for the tested molecules were obtained using Gaussian 09 software [42]. According to Pearson [43,44], the global hardness (η) and the fraction of electrons transferred (ΔN) from the surfactant to the iron surface are calculated according the following equations:

$$\Delta E_{gap} = E_{LUMO} - E_{HOMO} \quad (1)$$

$$\eta = \frac{\Delta E_{gap}}{2} = \frac{E_{LUMO} - E_{HOMO}}{2} \quad (2)$$

$$\Delta N = \frac{\phi - \chi_{inh}}{2(\eta_{Fe} - \eta_{inh})} \quad (3)$$

where ϕ , χ_{inh} , η_{Fe} and η_{inh} are the function work (4.82 eV), the electronegativity of the inhibitor, the chemical hardness of Fe(110) (0 eV) and the chemical hardness of the inhibitor, respectively.

values were inversely proportional to the cationic surfactant's concentration at low concentrations. At higher concentrations, the surface tension values were relatively stable. The critical micelle concentration (CMC) of a cationic surfactant is the concentration at the break. The CMC values for compounds **WA-1**, **WA-2** and **WA-3** at 298 K are 0.050, 0.062 and 0.069 mmol/L⁻¹, respectively. These values show that our novel peptidomimetic cationic surfactants have excellent micelle forming ability. The CMC values of compounds **WA-1**, **WA-2** and **WA-3** decreased with the increase in the alkyl chain length, which occurs because of the increase in the hydrophobicity of the investigated surfactant molecules with the raising of the length of the carbon chain. This increase in hydrophobicity leads to an increase in the mutual repulsion between the oppositely charged moieties, such as nonpolar hydrophobic carbon chains and polar water molecules. A great repulsion between the longer hydrophobic chain and the water phase reduced the CMC value[37,39]. The surface-active parameters of the cationic surfactants are summarized in **Table 1**.

<<<<<<**Figure 2**>>>>>>

<<<<<<**Table 1**>>>>>>

The value of the degree of counter ion dissociation (α) of the prepared cationic surfactants was calculated at 298 K. α was deduced from the specific electrical conductivity concentration curves and can be defined as the ratio between the premicellar and postmicellar slopes. The relationship between α and the degree of counter ion binding (β) is $\beta=1-\alpha$. The α values of synthesized peptidomimetic cationic surfactants **WA-3**, **WA-2** and **WA-1** at 25 °C were found to be 0.59, 0.55 and 0.53, respectively. As shown in **Table 1**, the specific electrical conductivity of the obtained surfactants was found to be inversely proportional to their hydrophobicity. Normally, the specific conductivity of cationic surfactants in an aqueous solution depends on the strength of the bond between the head of the surfactant and

their counter ion. All the numbers of counter ions were also found to be important parameters in determining the specific conductivity. To minimize the conductivity of the synthesized surfactant in aqueous solutions, we increased the hydrophobic chain length to decrease the number of water molecules around the hydrophilic head of the synthesized surfactant. Decreasing the hydration improved the density of the head charge, which increased the bond strength between their associated counterions and the surfactant's head. Consequently, the counter ion degree of dissociation has been reduced. Additionally, raising the molecular weight of the synthesized cationic surfactants by the increasing the length of the hydrophobic tail reduced the counterions' number and the electrical conductivity.[45–48]

The critical micelle concentrations (CMCs) of compounds **WA-1**, **WA-2**, and **WA-3** were determined at 25 °C by surface tension and electrical conductimetric techniques. The CMC values were obtained from the break point in the specific electrical conductivity versus concentration curve and in the surface tension- log[C] curve, as shown in **Fig. 2**.

The packing density of the surfactant molecules can be determined from the surface area (A_{min}) unavailable by the surfactant molecules at the interface of air-water [49]. The maximum surface excess (Γ_{max}) of the obtained surfactants is the surfactant unimer concentration in the interface/unit area (**Table 1**). The extreme surface excess (Γ_{max}) was calculated utilizing Gibb's adsorption equation **4**, as follows [50]:

$$\Gamma_{max} = \frac{-1}{2.303nRT} \left(\frac{d\gamma}{d \log C} \right)_T \quad (4)$$

where the gas constant is R , n is the number of ionic species ($n= 2$ for a mono-valent cationic surfactant), $(\delta \gamma / \delta \log c)$ is the slope below the CMC and the absolute temperature is T . Additionally, the minimum surface area (A_{min}) (in square angstrom) is known as the middling area occupied by each surfactant species adsorbed at the system interface. The A_{min} has been calculated at room temperature using Gibb's adsorption Eqn. [51].

$$A_{\min} = \frac{10^{14}}{\Gamma_{\max} \times N_A} \quad (5)$$

where N is Avogadro's number. As the hydrocarbon chain length increased from 10 to 16, we observed an increase in the value of Γ_{\max} and a decrease in the value of A_{\min} (**Table 1**). This clearly indicates that the synthesized cationic surfactant has a higher packing density. Although the hydrophilic group size is a major factor to determine the values of A_{\min} and Γ_{\max} , [52] the hydrophobic group's interactions increased by increasing the hydrocarbon chain length, which led to closer packing of the cationic surfactant molecules and, hence, increased the Γ_{\max} values. [53]

The effectiveness (Π_{CMC}) is calculated utilizing equation (6), and it is known as the difference between γ_0 (i.e., the value of the surface tension of distilled water) and γ_{CMC} (i.e., the CMC of the investigated surfactant).

$$\Pi_{CMC} = \gamma_0 - \gamma_{CMC} \quad (6)$$

All the values of Π_{CMC} are listed in **Table 1**, and they indicate that the synthesized cationic surfactants are highly effective in reducing the water surface tension. The dissolution of surfactant molecules is the main cause of the great water surface tension reduction [54].

The standard free energy changes of micellization (ΔG_{mic}^o) and adsorption (ΔG_{ads}^o) of the synthesized peptidomimetic cationic surfactants were calculated using the following eq. [23]:

$$\Delta G_{mic}^o = (2 - \alpha)RT \ln CMC \quad (7)$$

$$\Delta G_{ads}^o = (2 - \alpha)RT \ln CMC - 0.06\Pi_{CMC}A_{\min} \quad (8)$$

It can be inferred from the negative sign of the calculated thermodynamic parameters (**Table 1**) that the free energy of micellization and adsorption are both spontaneous processes. The ΔG_{mic}^o of our novel peptidomimetic cationic surfactants **WA-3**, **WA-2**, and **WA-1** were -

33.37, -34.80 and -35.27 kJ/mol, respectively. The ΔG_{ads}^0 of **WA-3**, **WA-2**, and **WA-1** were -37.08, -38.54 and -38.69 kJ/mol, respectively. From these data, it is noted that the micellization and adsorption processes increase by raising the hydrophobicity because of the increase in the repulsion between the polar aqueous solution and hydrocarbon group. This kind of change leads to disruption in the water structure, in which the surfactant molecule is dissolved and eventually leads to an increase in the system free energy. As expected, the surfactant molecules migrate to the interface or aggregate in micelles to reduce that repulsion process, and the free energy of the system consequently decreases[54].

3.3. Potentiodynamic polarization (PDP) experiments.

PDP experiments were carried out to investigate the influence of **WA-1**, **WA-2** and **WA-3** on the cathodic and anodic corrosion reactions of C-steel in 0.5 M hydrochloric acid solution. The polarization profiles in blank 0.5 M HCl and with various doses of the studied additives at 50 ° C are presented in Fig. 3. The addendum of all surfactants to the corrosive medium influenced the anodic, as well as the cathodic reactions, which indicate mixed type inhibitions. The values of the electrochemical parameters estimated from the polarization profiles, such as the cathodic and anode Tafel slopes (β_c, β_a), corrosion current density (I_{corr}), and corrosion potential (E_{corr}) are presented in Table 2. The protection power ($\eta\%$) was obtained from the I_{corr} values using the following eqn.[55]:

$$\eta / \% = \left(\frac{I_{corr}^o - I'_{corr}}{I_{corr}^o} \right) \times 100 \quad (9)$$

where I_{corr}^o and I'_{corr} are the I_{corr} of the uninhibited and inhibited systems, respectively. According to the previous studies,[56,57] if the modification in E_{corr} value is more than ± 85 mV in the solutions containing inhibitors related to blank system, the compound could be defined as a cathodic or anodic type inhibitor; if it is below ± 85 mV, it might be defined as the mixed type inhibitor. In this report, the supreme shifts in E_{corr} with the addition of **WA-1**,

WA-2 and **WA-3** were found to be 31, 30 and 7 mV, respectively, thus leading to the interpretation that the compounds behaved as mixed type inhibitors. It is noticed from Fig. 3 that the decrease in current density is greater at the cathode rather than at the anode, and the β_c values are greater than the β_a values, which suggests the predominance of cathodic inhibition.

<<<<<<**Figure 3**>>>>>>

<<<<<<**Table 2**>>>>>>

As shown in Table 2, the I_{corr} values in the presence of **WA-1**, **WA-2** and **WA-3** were higher than that of the uninhibited medium. The value of I_{corr} decreases from 2.189 mA cm⁻² to 0.15104 mA cm⁻² by means of **WA-3** to 0.05932 mA cm⁻² using **WA-2** and to 0.03831 mA cm⁻² in the presence of **WA-1** at 100 ppm. Consistently, the protection capacity rises with the surfactant dose, and the maximum values obtained for **WA-1**, **WA-2** and **WA-3** were observed to be 98.25%, 97.29% and 93.1%, respectively.

The increment in $\eta\%$ with increasing the surfactant dose could owe to a rise in the number of adsorbed molecules at metal/medium interface. The number of molecules that are adsorbed on the active sites on the metal surface increase with the increasing concentration the surfactant and lead to an increase in the coverage surface (θ) and $\eta\%$. The $\eta\%$ of carbon steel with **WA-1** was also higher than those of **WA-2** and **WA-3**. The values of $\eta\%$ at all investigated concentrations were rated as **WA-1** > **WA-2** > **WA-3**.

34. EIS data

The EIS spectra for C-steel in a 0.5 M solution of HCl with and without the occurrence of different amounts of the examined surfactants are presented by Nyquist diagrams and are exemplified in Fig. 4A, 4B and 4C for **WA-1**, **WA-2** and **WA-3**, respectively. The EIS spectra display analogous behavior in the inhibited and uninhibited

systems, which indicates that the C-steel corrosion inhibition in the HCl by the investigated inhibitors does not change the corrosion process mechanism.[58] The diameters of the semicircles of the Nyquist profiles with the occurrence of the surfactants are usually greater than those of the free inhibitors medium. This suggests the carbon steel/HCl interface shows greater impedance to charge movements in the presence of the studied compounds. This is suggestive of the protective action of the investigated inhibitors. Additionally, from Fig. 4, the Nyquist profile displays one depressed semicircle conformable to a single time constant. The Nyquist semicircle depression is due to frequency dispersal impacts that could be an outcome from the nonhomogeneity and coarseness of the surface of the electrode and/or further formulas of interstitial phenomena.[59]

<<<<<<Figure 4>>>>>>

The EIS data for the Nyquist plots was evaluated using the equivalent circuit routine, and the consistent equivalent circuit model (ECM) is depicted in Fig. 4D. In the ECM, R_s is the electrolyte resistance. The constant phase element (CPE) [60] for the metal/HCl interface model was applied in place of the “perfect” capacitance. R_{ct} represents the resistance of the charge transfer. The CPE impedance was stated as follows [58]:

$$Z_{CPE} = \frac{1}{Y_0(j\omega)^n} \quad (4)$$

where j represents the imaginary unit, Y_0 is the frequency independent admittance of CPE and ω characterizes the angular frequency. n is the exponent of CPE, which is generally close to 1. The CPE exponents were between 0.862 and 0.950, which designates a coarse medium on the steel surface. The C_{dl} was calculated by the following equation [61]:

$$C_{dl} = Y_0(\omega)^{n-1} = Y_0(2\pi f_{max})^{n-1} \quad (11)$$

where f_{max} is the frequency at which the maximum imaginary occurs on the Nyquist profiles in Fig. 4. The values of C_{dl} , R_{ct} , R_s , n and protection power ($\eta_E\%$) were estimated and

recorded in Table 3. The $\eta_E\%$ values of the inhibitors were intended from the R_{ct} values using the following eqn. [47]:

$$\eta_E / \% = 100 \times \left(\frac{R_{ct}^i - R_{ct}^0}{R_{ct}^i} \right) = 100 \times \theta \quad (12)$$

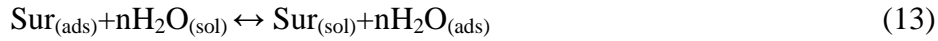
where R_{ct}^i and R_{ct}^0 are the R_{ct} in the inhibited and uninhibited systems. It is apparent from Table 3 that the R_{ct} value increases and the C_{dl} value decreases with the rise in the surfactant doses of all the studied additives. The maximum $\eta_E\%$ achieved at the optimum concentration of 100 ppm was found to be 96.96%, 95.36% and 92.38% for **WA-1**, **WA-2** and **WA-3**, respectively. These results are related to the development of a shielding film of the surfactant species on the electrode surface. The preventative layer of the surfactant diminishes the immediate approach of the C-steel with the corrosive medium.

<<<<<<Table 3>>>>>>>

According to the Helmholtz model,[62,63] the C_{dl} is inversely proportional to the protective layer intensity, which indicates that the decrease in C_{dl} demonstrates the rise in the intensity of the covering film with an increment in the inhibitor dose. Subsequently, the surfactant molecules replace more H_2O molecules of high dielectric constant present in the metal surface vicinity when inhibitor molecules with low dielectric constants are added in the HCl solution, which is indicative of reduction in the C_{dl} value. Additionally, the maximum inhibition was detected at 100 mg/L, which is in good correspondence with the data achieved from the PDP experiments.

3.5 Adsorption isotherms and corrosion inhibition mechanism

To provide more information regarding the corrosion inhibition mechanism, adsorption isotherm experiments were performed.[64] The surfactant molecule's trend to dislodge H_2O molecules from the steel interface in a reversible route is demonstrated via the following formula[65]:



where n represents the number of H_2O molecules. The adsorption performance of the examined surfactants was inspected by subjugation of the potentiodynamic polarization results into different adsorption models, such as the Temkin, Frumkin, Langmuir and Freundlich isotherms [65]. The results confirmed that the appropriate model was the Langmuir adsorption isotherm model, as follows:

$$\frac{C_{\text{inh}}}{\theta} = C_{\text{inh}} + \frac{1}{K_{\text{ads}}} \quad (14)$$

where C_{inh} is the [inhibitor], K_{ads} represents the equilibrium adsorption constant. The diagrams of C_{inh} versus C_{inh}/θ give a straight line, as presented in Fig. 5, and the K_{ads} values are obtained from the intercept. The straight-line relationship was obtained for the Temkin, Frumkin, Langmuir, and Freundlich isotherms with a correlation coefficient (R^2) over 0.8172. The Langmuir adsorption isotherm ($R^2 = 0.9996$) was found to be suitable for the experimental findings close to the Frumkin adsorption isotherm ($R^2 = 0.8542$), the Temkin adsorption isotherm ($R^2 = 0.9112$), and the Freundlich adsorption isotherm ($R^2 = 0.8172$). In addition, we mentioned that the slope of the Langmuir isotherm slightly deviated from the unity (i.e., 0.971 (**WA-1**), 0.979 (**WA-2**), and 0.997 (**WA-3**)) expected of an ideal Langmuir isotherm, which indicates the validity of Langmuir model [66]. The standard adsorption free energy (ΔG_{ads}^o) and K_{ads} are related by the equation given below:

$$K_{\text{ads}} = \frac{1}{55.5} \exp\left(-\frac{\Delta G_{\text{ads}}^o}{RT}\right) \quad (15)$$

The K_{ads} values obtained for the investigated inhibitors were high, i.e., 1.21×10^5 (**WA-1**), 1.001×10^5 (**WA-2**) and 7.14×10^4 (**WA-3**). The observations indicate the replacement of the H_2O species from the metal substrate by the surfactant molecules, and accordingly, the inhibitors adsorb powerfully on the surface of the steel. The trend of the ΔG_{ads}^o values is such

that **WA-1** ($-42.16 \text{ kJ mol}^{-1}$) > **WA-2** ($-41.51 \text{ kJ mol}^{-1}$) > **WA-3** ($-40.79 \text{ kJ mol}^{-1}$), which is the same as the relative order of the inhibition efficiency. The ΔG_{ads}^o values more than $-40.16 \text{ kJ mol}^{-1}$ indicate chemisorption.

<<<<<<**Figure 5**>>>>>>

3.6. DFT calculations

In the present work, we performed quantum calculations to find the relationship between the electronic features of the studied inhibitors and their experimental inhibition efficiencies. Recently, quantum calculations have been used to investigate the adsorption of new surfactants on the metallic interface [67,68].

The distribution density of the E_{HOMO} (i.e., the highest occupied molecular orbital), E_{LUMO} (i.e., the lowest unoccupied molecular orbital), in the gas phase, and MEP (i.e., the molecular electrostatic potential) are shown in Fig. 6. The HOMO density was localized on the chlorine atom and the LUMO density was distributed on the aromatic rings. Molecular electrostatic potential (MEP) is a method to analyze the reactive sites for nucleophilic and electrophilic attacks in the molecules. The red color shows the electrophilic reactivity, and the blue color shows the nucleophilic reactivity of the molecules (Fig. 6). Therefore, the most favorable sites for electrophilic attacks are the carbon atoms attached to chlorine and oxygen atoms where the negative regions are localized. Similarly, the most favorable sites for nucleophilic attack are the positive regions of the inhibitor. The quantum descriptors are listed in Table 4. The energies of HOMO and LUMO reflect the capability of the molecule to donate and to receive electrons to/from the vacant 3d-orbital of iron.[69,70]

<<<<<<**Figure 6**>>>>>>

Increasing the alkyl chain length caused an increase in the E_{HOMO} and a decrease in the E_{LUMO} values. Therefore, **WA-1** is predicted to have a corrosion inhibition activity higher than **WA-**

2 (Table 4). The energy gap (ΔE) value is associated with the stability of the synthesized inhibitor and the chemical reactivity of the complex between the metal and the inhibitor. The lower the value of ΔE , the higher the molecule's protection capacity. Therefore, **WA-1** is predicted to be a much better corrosion inhibitor than **WA-2**.

<<<<<<Table 4>>>>>>

The dipole moment (μ) results from the irregular distribution of charges on various atoms of the molecule.[71] A high dipole moment is desired to increase the adsorption of the molecule on metal surfaces.[72] The dipole moment of the **WA-1** molecule is higher than that of the **WA-2** molecule in the gas phase, which supports the prediction that the **WA-1** molecule has a higher corrosion inhibitor (Table 4). The dipole moments of **WA-1** and **WA-2** are not similar in the liquid and gas phases

We have also calculated the global hardness (η). The soft inhibitor is usually a highly reactive inhibitor that possess a lower ΔE value, and the opposite is true for the hard inhibitor.[73] Since the **WA-1** inhibitor has lower η value, this compound has a higher propensity to be adsorbed over the iron surface. We calculated the fraction of electrons that is transferred from the inhibitor molecule to the steel interface (ΔN) using Pearson's formula (Eq. 3). The inhibitor molecules having higher ΔN values easily transfer electrons to the unoccupied d-orbital of the metal interface. The electron donation of the **WA-1** inhibitors was found to be higher than that of **WA-2**.

3.7. MD simulations

The interaction between the inhibitors and the iron surface was simulated using the Monte Carlo method and was calculated by the following relation (16):

$$E_{\text{int}} = E_{\text{tot}} - (E_{\text{Fe}} + E_{\text{inh}}) \quad (16)$$

4. Conclusions

In the present work, experimental and theoretical approaches were used to study the protection actions of three novel peptidomimetic cationic surfactants on C-steel corrosion. All the examined peptidomimetic cationic surfactants act as good additives for carbon steel erosion, and their protection capacity increased with the increase in their concentration. The combination of peptidomimetic moiety with a long alkyl chain improved the anti-corrosion properties of the studied compounds. The studied peptidomimetic compounds showed a protection power of 98.25% at 0.17 mM (at 0.5 M HCl and 50 °C temperature). The PDP studies revealed that the new peptidomimetic surfactants behaved as mixed type inhibitors. The impedance showed increases in the R_{ct} values due to the adsorption of additives on the steel/medium interfaces following the Langmuir model and comprises chemisorption action. The DFT calculations were found to be in agreement with the experimental findings. The MD simulations demonstrated that the compounds adsorb powerfully on the iron (110) interface by parallel or flat modes, and the E_{binding} trend agrees with the obtained protection capacity. This study introduced novel peptidomimetic compounds as a new class of cationic surfactants that could be useful in the field of anti-corrosion applications.

Declaration of Competing Interest

The authors declare that they have no known competing financial interests or personal relationships that could have appeared to influence the work reported in this paper.

References

- [1] M. Heydari, M. Javidi, Corrosion inhibition and adsorption behaviour of an amido-imidazoline derivative on API 5L X52 steel in CO₂-saturated solution and synergistic effect of iodide ions, *Corros. Sci.* 61 (2012) 148–155. <https://doi.org/10.1016/j.corsci.2012.04.034>.
- [2] D.M. Ortega-Toledo, J.G. Gonzalez-Rodriguez, M. Casales, L. Martinez, A. Martinez-

- Villafañe, Co₂ corrosion inhibition of X-120 pipeline steel by a modified imidazoline under flow conditions, *Corros. Sci.* 53 (2011) 3780–3787. <https://doi.org/10.1016/j.corsci.2011.07.028>.
- [3] M.W.S. Jawich, G.A. Oweimreen, S.A. Ali, Heptadecyl-tailed mono- and bis-imidazolines: A study of the newly synthesized compounds on the inhibition of mild steel corrosion in a carbon dioxide-saturated saline medium, *Corros. Sci.* 65 (2012) 104–112. <https://doi.org/10.1016/j.corsci.2012.08.001>.
- [4] H.M. Abd El-Lateef, Corrosion inhibition characteristics of a novel salicylidene isatin hydrazine sodium sulfonate on carbon steel in HCl and a synergistic nickel ions additive: A combined experimental and theoretical perspective, *Appl. Surf. Sci.* 501 (2020) 144237. <https://doi.org/10.1016/j.apsusc.2019.144237>.
- [5] H.M. Abd El-Lateef, A.O. Alnajjar, Enhanced the protection capacity of poly(o-toluidine) by synergism with zinc or lanthanum additives at C-steel/HCl interface: A combined DFT, molecular dynamic simulations and experimental methods, *J. Mol. Liq.* 303 (2020) 112641. <https://doi.org/10.1016/j.molliq.2020.112641>.
- [6] H.M.A. El-Lateef, Z.A. Abdallah, M.S.M. Ahmed, Solvent-free synthesis and corrosion inhibition performance of Ethyl 2-(1,2,3,6-tetrahydro-6-oxo-2-thioxopyrimidin-4-yl)ethanoate on carbon steel in pickling acids: Experimental, quantum chemical and Monte Carlo simulation studies, *J. Mol. Liq.* 296 (2019) 111800. <https://doi.org/10.1016/j.molliq.2019.111800>.
- [7] M. Abdallah, M.A. Hegazy, M. Alfakeer, H. Ahmed, Adsorption and inhibition performance of the novel cationic gemini surfactant as a safe corrosion inhibitor for carbon steel in hydrochloric acid, *Green Chem. Lett. Rev.* 11 (2018) 457–468. <https://doi.org/10.1080/17518253.2018.1526331>.
- [8] I. Aiad, S.M. Shaban, H.Y. Moustafa, A. Hamed, Experimental investigation of newly

- synthesized gemini cationic surfactants as corrosion inhibitors of mild steel in 1.0 M HCl, *Prot. Met. Phys. Chem. Surfaces.* 54 (2018) 135–147. <https://doi.org/10.1134/S2070205118010173>.
- [9] M. Mahdavian, A.R. Tehrani-Bagha, E. Alibakhshi, S. Ashhari, M.J. Palimi, S. Farashi, S. Javadian, F. Ektefa, Corrosion of mild steel in hydrochloric acid solution in the presence of two cationic gemini surfactants with and without hydroxyl substituted spacers, *Corros. Sci.* 137 (2018) 62–75. <https://doi.org/10.1016/j.corsci.2018.03.034>.
- [10] M.A. Deyab, Efficiency of cationic surfactant as microbial corrosion inhibitor for carbon steel in oilfield saline water, *J. Mol. Liq.* 255 (2018) 550–555. <https://doi.org/10.1016/j.molliq.2018.02.019>.
- [11] A.H. Tantawy, K.A. Soliman, H.M. Abd El-Lateef, Novel synthesized cationic surfactants based on natural piper nigrum as sustainable-green inhibitors for steel pipeline corrosion in CO₂-3.5%NaCl: DFT, Monte Carlo simulations and experimental approaches, *J. Clean. Prod.* (2019) 119510. <https://doi.org/10.1016/j.jclepro.2019.119510>.
- [12] C.A.J. Richards, H.N. McMurray, G. Williams, Smart-release inhibition of corrosion driven organic coating failure on zinc by cationic benzotriazole based pigments, *Corros. Sci.* 154 (2019) 101–110. <https://doi.org/10.1016/j.corsci.2019.04.005>.
- [13] K. Shalabi, A.M. Helmy, A.H. El-Askalany, M.M. Shahba, New pyridinium bromide mono-cationic surfactant as corrosion inhibitor for carbon steel during chemical cleaning: Experimental and theoretical studies, *J. Mol. Liq.* 293 (2019). <https://doi.org/10.1016/j.molliq.2019.111480>.
- [14] S.A. Umoren, M.M. Solomon, Effect of halide ions on the corrosion inhibition efficiency of different organic species - A review, *J. Ind. Eng. Chem.* 21 (2015) 81–100. <https://doi.org/10.1016/j.jiec.2014.09.033>.

- [15] M. Gao, J. Zhang, Q. Liu, J. Li, R. Zhang, G. Chen, Effect of the alkyl chain of quaternary ammonium cationic surfactants on corrosion inhibition in hydrochloric acid solution, *Comptes Rendus Chim.* 22 (2019) 355–362. <https://doi.org/10.1016/j.crci.2019.03.006>.
- [16] A. Pinazo, M.A. Manresa, A.M. Marques, M. Bustelo, M.J. Espuny, L. Pérez, Amino acid-based surfactants: New antimicrobial agents, *Adv. Colloid Interface Sci.* 228 (2016) 17–39. <https://doi.org/10.1016/j.cis.2015.11.007>.
- [17] S.M. Rajput, S. Kumar, V.K. Aswal, O.A. El Seoud, N.I. Malek, S.K. Kailasa, Drug-Induced Micelle-to-Vesicle Transition of a Cationic Gemini Surfactant: Potential Applications in Drug Delivery, *ChemPhysChem.* 19 (2018) 865–872. <https://doi.org/10.1002/cphc.201701134>.
- [18] R. Muzzalupo, L. Pérez, A. Pinazo, L. Tavano, Pharmaceutical versatility of cationic niosomes derived from amino acid-based surfactants: Skin penetration behavior and controlled drug release, *Int. J. Pharm.* 529 (2017) 245–252. <https://doi.org/10.1016/j.ijpharm.2017.06.083>.
- [19] C. Botto, N. Mauro, E. Amore, E. Martorana, G. Giammona, M.L. Bondì, Surfactant effect on the physicochemical characteristics of cationic solid lipid nanoparticles, *Int. J. Pharm.* 516 (2017) 334–341. <https://doi.org/10.1016/j.ijpharm.2016.11.052>.
- [20] L. Wang, P. Quan, S.H. Chen, W. Bu, Y.-F. Li, X. Wu, J. Wu, L. Zhang, Y. Zhao, X. Jiang, B. Lin, R. Zhou, C. Chen, Stability of Ligands on Nanoparticles Regulating the Integrity of Biological Membranes at the Nano–Lipid Interface, *ACS Nano.* 13 (2019) 8680–8693. <https://doi.org/10.1021/acsnano.9b00114>.
- [21] L. Wang, Q. Zhao, Z. Zhang, Z. Lu, Y. Zhao, Y. Tang, Fluorescent Conjugated Polymer/Quaternary Ammonium Salt Co-assembly Nanoparticles: Applications in Highly Effective Antibacteria and Bioimaging, *ACS Appl. Bio Mater.* 1 (2018) 1478–

1486. <https://doi.org/10.1021/acsabm.8b00422>.
- [22] E. Paluch, A. Piecuch, E. Obłąk, Lamch, K.A. Wilk, Antifungal activity of newly synthesized chemodegradable dicephalic-type cationic surfactants, *Colloids Surfaces B Biointerfaces*. 164 (2018) 34–41. <https://doi.org/10.1016/j.colsurfb.2018.01.020>.
- [23] K. Kani, M.B. Zakaria, J. Lin, A.A. Alshehri, J. Kim, Y. Bando, J. You, M.S.A. Hossain, J. Bo, Y. Yamauchi, Synthesis and Characterization of Dendritic Pt Nanoparticles by Using Cationic Surfactant, *Bull. Chem. Soc. Jpn.* 91 (2018) 1333–1336. <https://doi.org/10.1246/bcsj.20180129>.
- [24] N.J. Buurma, Aggregation and reactivity in aqueous solutions of cationic surfactants and aromatic anions across concentration scales, *Curr. Opin. Colloid Interface Sci.* 32 (2017) 69–75. <https://doi.org/10.1016/j.cocis.2017.10.005>.
- [25] H. Nourmoradi, A. Daneshfar, S. Mazloomi, J. Bagheri, S. Barati, Removal of Penicillin G from aqueous solutions by a cationic surfactant modified montmorillonite, *MethodsX*. 6 (2019) 1967–1973. <https://doi.org/10.1016/j.mex.2019.08.019>.
- [26] A. dos Santos, M.F. Viante, D.J. Pochapski, A.J. Downs, C.A.P. Almeida, Enhanced removal of p-nitrophenol from aqueous media by montmorillonite clay modified with a cationic surfactant, *J. Hazard. Mater.* 355 (2018) 136–144. <https://doi.org/10.1016/j.jhazmat.2018.02.041>.
- [27] E. Piperopoulos, E. Mastronardo, M. Fazio, M. Lanza, S. Galvagno, C. Milone, Enhancing the volumetric heat storage capacity of Mg(OH)₂ by the addition of a cationic surfactant during its synthesis, *Appl. Energy*. 215 (2018) 512–522. <https://doi.org/10.1016/j.apenergy.2018.02.047>.
- [28] Q. Guo, Z. Zhang, Y. Song, S. Liu, W. Gao, H. Qiao, L. Guo, J. Wang, Investigation on interaction of DNA and several cationic surfactants with different head groups by spectroscopy, gel electrophoresis and viscosity technologies, *Chemosphere*. 168

- (2017) 599–605. <https://doi.org/10.1016/j.chemosphere.2016.11.019>.
- [29] L.Y. Zakharova, G.I. Kaupova, D.R. Gabdrakhmanov, G.A. Gaynanova, E.A. Ermakova, A.R. Mukhitov, I. V. Galkina, S. V. Cheresiz, A.G. Pokrovsky, P. V. Skvortsova, Y. V. Gogolev, Y.F. Zuev, Alkyl triphenylphosphonium surfactants as nucleic acid carriers: complexation efficacy toward DNA decamers, interaction with lipid bilayers and cytotoxicity studies, *Phys. Chem. Chem. Phys.* 21 (2019) 16706–16717. <https://doi.org/10.1039/c9cp02384d>.
- [30] M. López-López, P. López-Cornejo, V.I. Martín, F.J. Ostos, C. Checa-Rodríguez, R. Prados-Carvajal, J.A. Lebrón, P. Huertas, M.L. Moyá, Importance of hydrophobic interactions in the single-chained cationic surfactant-DNA complexation, *J. Colloid Interface Sci.* 521 (2018) 197–205. <https://doi.org/10.1016/j.jcis.2018.03.048>.
- [31] C. Zhou, F. Wang, H. Chen, M. Li, F. Qiao, Z. Liu, Y. Hou, C. Wu, Y. Fan, L. Liu, S. Wang, Y. Wang, Selective Antimicrobial Activities and Action Mechanism of Micelles Self-Assembled by Cationic Oligomeric Surfactants, *ACS Appl. Mater. Interfaces.* 8 (2016) 4242–4249. <https://doi.org/10.1021/acsami.5b12688>.
- [32] V. Castelletto, R.H. Barnes, K.A. Karatzas, C.J.C. Edwards-Gayle, F. Greco, I.W. Hamley, R. Rambo, J. Seitsonen, J. Ruokolainen, Arginine-Containing Surfactant-Like Peptides: Interaction with Lipid Membranes and Antimicrobial Activity, *Biomacromolecules.* 19 (2018) 2782–2794. <https://doi.org/10.1021/acs.biomac.8b00391>.
- [33] B.J.H. Banaschewski, E.J.A. Veldhuizen, E. Keating, H.P. Haagsman, Y.Y. Zuo, C.M. Yamashita, R.A.W. Veldhuizen, Antimicrobial and biophysical properties of surfactant supplemented with an antimicrobial peptide for treatment of bacterial pneumonia, *Antimicrob. Agents Chemother.* 59 (2015) 3075–3083. <https://doi.org/10.1128/AAC.04937-14>.

- [34] I.W. Hamley, J. Hutchinson, S. Kirkham, V. Castelletto, A. Kaur, M. Reza, J. Ruokolainen, Nanosheet Formation by an Anionic Surfactant-like Peptide and Modulation of Self-Assembly through Ionic Complexation, *Langmuir*. 32 (2016) 10387–10393. <https://doi.org/10.1021/acs.langmuir.6b02180>.
- [35] S. Gheorghe, I. Lucaciu, I. Paun, C. Stoica, E. Stanescu, Ecotoxicological Behavior of some Cationic and Amphoteric Surfactants (Biodegradation, Toxicity and Risk Assessment), in: *Biodegrad. - Life Sci., InTech*, 2013. <https://doi.org/10.5772/56199>.
- [36] N.A. Negm, F.M. Ghuiba, S.M. Tawfik, Novel isoxazolium cationic Schiff base compounds as corrosion inhibitors for carbon steel in hydrochloric acid, *Corros. Sci.* 53 (2011) 3566–3575. <https://doi.org/10.1016/j.corsci.2011.06.029>.
- [37] H.M. Abd El-Lateef, A.H. Tantawy, Synthesis and evaluation of novel series of Schiff base cationic surfactants as corrosion inhibitors for carbon steel in acidic/chloride media: Experimental and theoretical investigations, *RSC Adv.* 6 (2016) 8681–8700. <https://doi.org/10.1039/c5ra21626e>.
- [38] M. Crawford, W.T. Little, 145. The Erlenmeyer reaction with aliphatic aldehydes, 2-phenyloxazol-5-one being used instead of hippuric acid, *J. Chem. Soc.* 0 (1959) 729. <https://doi.org/10.1039/jr9590000729>.
- [39] H.M. Abd El-Lateef, K.A. Soliman, A.H. Tantawy, Novel synthesized Schiff Base-based cationic gemini surfactants: Electrochemical investigation, theoretical modeling and applicability as biodegradable inhibitors for mild steel against acidic corrosion, *J. Mol. Liq.* 232 (2017) 478–498. <https://doi.org/10.1016/j.molliq.2017.02.105>.
- [40] C. Lee, W. Yang, R.G. Parr, Development of the Colle-Salvetti correlation-energy formula into a functional of the electron density, *Phys. Rev. B.* 37 (1988) 785–789. <https://doi.org/10.1103/PhysRevB.37.785>.
- [41] M. Cossi, N. Rega, G. Scalmani, V. Barone, Energies, structures, and electronic

- properties of molecules in solution with the C-PCM solvation model, *J. Comput. Chem.* 24 (2003) 669–681. <https://doi.org/10.1002/jcc.10189>.
- [42] D.J.F. 25. M. J. Frisch, G. W. Trucks, H. B. Schlegel, G. E. Scuseria, M. A. Robb, J. R. Cheeseman, G. Scalmani, V. Barone, B. Mennucci, G. A. Petersson, H. Nakatsuji, M. Caricato, X. Li, H. P. Hratchian, A. F. Izmaylov, J. Bloino, G. Zheng, J. L. Sonnenberg, M., Gaussian, Inc., Wallingford CT, (2010).
- [43] R.G. Pearson, Absolute Electronegativity and Hardness: Application to Inorganic Chemistry, *Inorg. Chem.* 27 (1988) 734–740. <https://doi.org/10.1021/ic00277a030>.
- [44] R.G. Pearson, Hard and soft acids and bases-the evolution of a chemical concept, *Coord. Chem. Rev.* 100 (1990) 403–425. [https://doi.org/10.1016/0010-8545\(90\)85016-L](https://doi.org/10.1016/0010-8545(90)85016-L).
- [45] R. Li, F. Yan, J. Zhang, C. Xu, J. Wang, The self-assembly properties of a series of polymerizable cationic gemini surfactants: Effect of the acryloxyl group, *Colloids Surfaces A Physicochem. Eng. Asp.* 444 (2014) 276–282. <https://doi.org/10.1016/j.colsurfa.2013.12.079>.
- [46] B. Kumar, D. Tikariha, K.K. Ghosh, P. Quagliotto, Effect of short chain length alcohols on micellization behavior of cationic gemini and monomeric surfactants, *J. Mol. Liq.* 172 (2012) 81–87. <https://doi.org/10.1016/j.molliq.2012.05.013>.
- [47] H.M. Abd El-Lateef, A.H. Tantawy, A.A. Abdelhamid, Novel Quaternary Ammonium-Based Cationic Surfactants: Synthesis, Surface Activity and Evaluation as Corrosion Inhibitors for C1018 Carbon Steel in Acidic Chloride Solution, *J. Surfactants Deterg.* 20 (2017) 735–753. <https://doi.org/10.1007/s11743-017-1947-7>.
- [48] A. Laschewsky, L. Wattebled, M. Arotçaréna, J.L. Habib-Jiwan, R.H. Rakotoaly, Synthesis and properties of cationic oligomeric surfactants, *Langmuir.* 21 (2005) 7170–7179. <https://doi.org/10.1021/la050952o>.

- [49] W. Qiao, J. Li, H. Peng, Y. Zhu, H. Cai, Synthesis of single and double long-chain 1,3,5-triazine amphoteric surfactants and their surface activity, *Colloids Surfaces A Physicochem. Eng. Asp.* 384 (2011) 612–617. <https://doi.org/10.1016/j.colsurfa.2011.05.008>.
- [50] M.J. Rosen, J.T. Kunjappu, *Surfactants and Interfacial Phenomena: Fourth Edition*, John Wiley and Sons, Hoboken, NJ, USA, 2012. <https://doi.org/10.1002/9781118228920>.
- [51] Y. Zhao, X. Yue, X. Wang, D. Huang, X. Chen, Micelle formation by N-alkyl-N-methylpiperidinium bromide ionic liquids in aqueous solution, *Colloids Surfaces A Physicochem. Eng. Asp.* 412 (2012) 90–95. <https://doi.org/10.1016/j.colsurfa.2012.07.021>.
- [52] B. Dong, X. Zhao, L. Zheng, J. Zhang, N. Li, T. Inoue, Aggregation behavior of long-chain imidazolium ionic liquids in aqueous solution: Micellization and characterization of micelle microenvironment, *Colloids Surfaces A Physicochem. Eng. Asp.* 317 (2008) 666–672. <https://doi.org/10.1016/j.colsurfa.2007.12.001>.
- [53] Y. Bao, J. Guo, J. Ma, P. Liu, Q. Kang, J. Zhang, Cationic silicon-based gemini surfactants: Effect of hydrophobic chains on surface activity, physico-chemical properties and aggregation behaviors, *J. Ind. Eng. Chem.* 53 (2017) 51–61. <https://doi.org/10.1016/j.jiec.2017.03.045>.
- [54] H. Li, C. Yu, R. Chen, J. Li, J. Li, Novel ionic liquid-type Gemini surfactants: Synthesis, surface property and antimicrobial activity, *Colloids Surfaces A Physicochem. Eng. Asp.* 395 (2012) 116–124. <https://doi.org/10.1016/j.colsurfa.2011.12.014>.
- [55] N.M. El Basiony, A. Elgendy, H. Nady, M.A. Migahed, E.G. Zaki, Adsorption characteristics and inhibition effect of two Schiff base compounds on corrosion of mild

- steel in 0.5 M HCl solution: Experimental, DFT studies, and Monte Carlo simulation, *RSC Adv.* 9 (2019) 10473–10485. <https://doi.org/10.1039/c9ra00397e>.
- [56] M.A. Hegazy, A.A. Nazeer, K. Shalabi, Electrochemical studies on the inhibition behavior of copper corrosion in pickling acid using quaternary ammonium salts, *J. Mol. Liq.* 209 (2015) 419–427. <https://doi.org/10.1016/j.molliq.2015.05.043>.
- [57] A.S. El-Tabei, M.A. Hegazy, Application of the Synthesized Novel 3,6,9,12,15,18,21-heptaooxatricosane-1,23-diyl bis(4-((4-(dimethylamino)benzylidene)amino)benzoate) as a Corrosion Inhibitor for Carbon Steel in Acidic Media, *J. Dispers. Sci. Technol.* 35 (2014) 1289–1299. <https://doi.org/10.1080/01932691.2013.838177>.
- [58] L.O. Olasunkanmi, I.B. Obot, E.E. Ebenso, Adsorption and corrosion inhibition properties of: N -{ n -[1-R-5-(quinoxalin-6-yl)-4,5-dihydropyrazol-3-yl]phenyl}methanesulfonamides on mild steel in 1 M HCl: Experimental and theoretical studies, *RSC Adv.* 6 (2016) 86782–86797. <https://doi.org/10.1039/c6ra11373g>.
- [59] A. Al-Amiery, A. Kadhum, A. Mohamad, A. Musa, C. Li, Electrochemical Study on Newly Synthesized Chlorocurcumin as an Inhibitor for Mild Steel Corrosion in Hydrochloric Acid, *Materials (Basel)*. 6 (2013) 5466–5477. <https://doi.org/10.3390/ma6125466>.
- [60] N. Labjar, M. Lebrini, F. Bentiss, N.E. Chihib, S. El Hajjaji, C. Jama, Corrosion inhibition of carbon steel and antibacterial properties of aminotris-(methylenephosphonic) acid, *Mater. Chem. Phys.* 119 (2010) 330–336. <https://doi.org/10.1016/j.matchemphys.2009.09.006>.
- [61] S.H. Yoo, Y.W. Kim, K. Chung, N.K. Kim, J.S. Kim, Corrosion inhibition properties of triazine derivatives containing carboxylic acid and amine groups in 1.0 M HCl solution, *Ind. Eng. Chem. Res.* 52 (2013) 10880–10889.

- <https://doi.org/10.1021/ie303092j>.
- [62] D.G. Ladha, P.M. Wadhvani, S. Kumar, N.K. Shah, Evaluation of corrosion inhibitive properties of *Trigonella foenum-graecum* for pure Aluminium in hydrochloric acid, *J. Mater. Environ. Sci.* 6 (2015) 1200–1209.
- [63] D.G. Ladha, P.M. Wadhvani, M.Y. Lone, P.C. Jha, N.K. Shah, Evaluation of fennel seed extract as a green corrosion inhibitor for pure aluminum in hydrochloric acid: An experimental and computational approach, *Anal. Bioanal. Electrochem.* 7 (2015) 59–74. <https://www.magiran.com/paper/1379044?lang=en> (accessed April 4, 2020).
- [64] P. Morales-Gil, G. Negrón-Silva, M. Romero-Romo, C. Ángeles-Chávez, M. Palomar-Pardavé, Corrosion inhibition of pipeline steel grade API 5L X52 immersed in a 1 M H₂SO₄ aqueous solution using heterocyclic organic molecules, *Electrochim. Acta.* 49 (2004) 4733–4741. <https://doi.org/10.1016/j.electacta.2004.05.029>.
- [65] L.O. Olasunkanmi, I.B. Obot, M.M. Kabanda, E.E. Ebenso, Some quinoxalin-6-yl derivatives as corrosion inhibitors for mild steel in hydrochloric acid: Experimental and theoretical studies, *J. Phys. Chem. C.* 119 (2015) 16004–16019. <https://doi.org/10.1021/acs.jpcc.5b03285>.
- [66] M. Behpour, S.M. Ghoreishi, N. Soltani, M. Salavati-Niasari, M. Hamadani, A. Gandomi, Electrochemical and theoretical investigation on the corrosion inhibition of mild steel by thiosalicylaldehyde derivatives in hydrochloric acid solution, *Corros. Sci.* 50 (2008) 2172–2181. <https://doi.org/10.1016/j.corsci.2008.06.020>.
- [67] A. Elgendy, A.E. Elkholy, N.M. El Basiony, M.A. Migahed, Monte Carlo simulation for the antiscaling performance of Gemini ionic liquids, *J. Mol. Liq.* 285 (2019) 408–415. <https://doi.org/10.1016/j.molliq.2019.04.117>.
- [68] M.A. Migahed, A. Elgendy, M.M. EL-Rabiei, H. Nady, E.G. Zaki, Novel Gemini cationic surfactants as anti-corrosion for X-65 steel dissolution in oilfield produced

- water under sweet conditions: Combined experimental and computational investigations, *J. Mol. Struct.* 1159 (2018) 10–22. <https://doi.org/10.1016/j.molstruc.2018.01.033>.
- [69] Z. Shariatnia, A. Ahmadi-Ashtiani, Corrosion inhibition efficiency of some phosphoramidate derivatives: DFT computations and MD simulations, *J. Mol. Liq.* 292 (2019) 111409. <https://doi.org/10.1016/j.molliq.2019.111409>.
- [70] N. Ammouchi, H. Allal, E. Zouaoui, K. Dob, D. Zouied, M. Bououdina, Extracts of *Ruta chalepensis* as green corrosion inhibitor for copper CDA 110 in 3% NaCl medium: Experimental and theoretical studies, *Anal. Bioanal. Electrochem.* 11 (2019) 830–850. <https://www.magiran.com/paper/2014790/?lang=en> (accessed April 4, 2020).
- [71] O. Kikuchi, Systematic QSAR Procedures with Quantum Chemical Descriptors, *Quant. Struct. Relationships.* 6 (1987) 179–184. <https://doi.org/10.1002/qsar.19870060406>.
- [72] X. Li, S. Deng, H. Fu, T. Li, Adsorption and inhibition effect of 6-benzylaminopurine on cold rolled steel in 1.0 M HCl, *Electrochim. Acta.* 54 (2009) 4089–4098. <https://doi.org/10.1016/j.electacta.2009.02.084>.
- [73] N.K. Allam, Thermodynamic and quantum chemistry characterization of the adsorption of triazole derivatives during Muntz corrosion in acidic and neutral solutions, *Appl. Surf. Sci.* 253 (2007) 4570–4577. <https://doi.org/10.1016/j.apsusc.2006.10.008>.
- [74] H. Hamitouche, A. Khelifa, A. Kouache, S. Moulay, Petroleum quaternary ammonium surfactants mixture synthesized from light naphtha as corrosion inhibitors for carbon steel in 1 m HCl, *Corros. Rev.* 31 (2013) 61–72. <https://doi.org/10.1515/correv-2012-0022>.

- [75] M.A. Hegazy, A.S. El-Tabei, A.H. Bedair, M.A. Sadeq, Synthesis and inhibitive performance of novel cationic and gemini surfactants on carbon steel corrosion in 0.5 M H₂SO₄ solution, RSC Adv. 5 (2015) 64633–64650. <https://doi.org/10.1039/c5ra06473b>.
- [76] M.A. Hegazy, A novel Schiff base-based cationic gemini surfactants: Synthesis and effect on corrosion inhibition of carbon steel in hydrochloric acid solution, Corros. Sci. 51 (2009) 2610–2618. <https://doi.org/10.1016/j.corsci.2009.06.046>.
- [77] S.M. Shaban, N-(3-(Dimethyl benzyl ammonio)propyl)alkanamide chloride derivatives as corrosion inhibitors for mild steel in 1 M HCl solution: Experimental and theoretical investigation, RSC Adv. 6 (2016) 39784–39800. <https://doi.org/10.1039/c6ra00252h>.

LIST OF TABLES

No.	Caption
TABLE 1	Surface-active properties of the synthesized cationic surfactant compounds (WA-1, WA-2 and WA-3)
TABLE 2	Electrochemical parameters and inhibition efficiency obtained from polarization measurements for carbon steel in 0.5 M HCl in the absence and presence of various concentrations of investigated inhibitors at 50 °C.
TABLE 3	Electrochemical impedance parameters for carbon steel in 0.5 M HCl containing various concentrations of the synthesized surfactants at 50 °C.
TABLE 4	The calculated quantum chemical descriptors in gas phase, the values in brackets for liquid phase and Interaction energy and binding energy values between the Fe (110) plane and studied compounds
TABLE 5	Comparative chart listing the performance of cationic surfactants-based corrosion inhibitors

Table 1:

Compounds	CMC ^a / mM L ⁻¹	CMC ^b / mM L ⁻¹	γ_{CMC} / mN m ⁻¹	π_{CMC} / mN m ⁻¹	α	β	Γ_{max} / $\mu\text{mol/m}^{-2}$	A_{min} / nm ²	$\Delta G_{\text{mic}}^{\circ}$ / KJ mol ⁻¹	$\Delta G_{\text{ads}}^{\circ}$ / KJ mol ⁻¹
WA1	0.050	0.053	37.82	34.18	0.53	0.47	9.94	1.67	-35.27	-38.69
WA2	0.062	0.064	39.62	32.38	0.55	0.45	8.59	1.93	-34.80	-38.54
WA3	0.069	0.071	44.14	27.86	0.59	0.41	7.46	2.22	-33.37	-37.08

^a CMC values obtained from surface tension measurements

^b CMC values obtained from conductivity measurements

Table 2:

Inhibitors code	C_{inh} / ppm by weight	I_{corr} / $\mu A cm^{-2}$ \pm SD	$-E_{corr}$ / mV (SCE)	β_a / mV dec ⁻¹	$-\beta_c$ / mV dec ⁻¹	θ	η_{PDP} / %
Blank	0.0	2189\pm125	440	124	202	-	-
WA-1	10	613.3 \pm 51	440	129	216	0.719	71.98
	25	407.1 \pm 32	447	132	198	0.814	81.40
	50	190.8 \pm 15	435	131	208	0.912	91.28
	75	104.4 \pm 9	427	130	210	0.952	95.23
	100	38.3 \pm 3	434	131	214	0.982	98.25
WA-2	10	692.6 \pm 53	466	131	214	0.683	68.36
	25	509.8 \pm 35	470	136	208	0.767	76.71
	50	253.1 \pm 27	439	131	201	0.884	88.44
	75	139.8 \pm 11	465	131	203	0.936	93.61
	100	59.3 \pm 4	470	135	207	0.972	97.29
WA-3	10	784.9 \pm 62	451	126	199	0.641	64.14
	25	647.9 \pm 56	471	131	212	0.704	70.40
	50	354.2 \pm 21	431	128	215	0.838	83.82
	75	223.1 \pm 14	456	129	191	0.898	89.81
	100	151.1 \pm 7	468	134	207	0.931	93.10

Table 3:

Inhibitors code	C_{inh} / ppm by weight	R_{ct} / $\Omega \text{ cm}^2$ $\pm \text{SD}$	C_{dl} / $\mu\text{F cm}^{-2}$	Q_{CPE}		θ	$\eta_{EIS}/\%$
				Y_0 / $\mu\Omega^{-1} \text{ s}^n \text{ cm}^{-2}$	n		
Blank	0.0	13.1±1.1	151.37	4.88	0.7647	--	--
WA-1	10	41.2±2.5	35.97	1.19	0.892	0.681	68.15
	25	84.1±5.6	27.39	0.73	0.901	0.844	84.39
	50	162.9±11.2	11.63	0.49	0.892	0.919	91.94
	75	312.1±22.7	6.13	0.26	0.931	0.957	95.79
	100	431.6±26.8	4.23	0.14	0.950	0.969	96.96
WA-2	10	35.6±2.3	46.52	1.54	0.872	0.631	63.14
	25	54.3±4.8	30.99	0.93	0.862	0.758	75.83
	50	92.5±7.4	14.62	0.64	0.882	0.858	85.81
	75	142.7±12.1	9.09	0.32	0.892	0.908	90.80
	100	282.8±14.9	5.81	0.17	0.911	0.953	95.36
WA-3	10	30.8±1.9	62.15	2.01	0.862	0.574	57.40
	25	37.5±2.6	44.56	1.22	0.872	0.650	65.01
	50	77.4±5.3	24.24	0.84	0.882	0.830	83.04
	75	101.4±6.7	15.28	0.43	0.892	0.870	87.06
	100	172.3±11.5	8.44	0.23	0.901	0.923	92.38

Table 4:

Inhibitors code	$E_{\text{HOMO}}/$ eV	$E_{\text{LUMO}}/$ eV	$\Delta E/$ eV	μ/Debye	η/eV	$\Delta N/e$	$E_{\text{int}} /$ kcal/mol	$E_{\text{binding}} /$ kcal/mol
WA2	-5.75 (-5.96)	-1.74 (-1.84)	4.01 (4.12)	4.655 (11.88)	2.005 (2.060)	0.266 (0.223)	-192.59	192.59
WA1	-5.74 (-5.95)	-1.75 (-1.84)	3.99 (4.11)	4.669 (11.60)	1.995 (2.055)	0.268 (0.224)	-199.12	199.12

Table 5

Inhibitor	Metal or alloy	Corrosive medium/	inhibitor dose	The protection power $\eta\%$	References
Petroleum quaternary ammonium surfactants	carbon steel	1.0 M HCl	560 ppm	84	[74]
((Z)-1-dodecyl-2- (2-hydroxybenzylideneamino) pyridinium bromide)	carbon steel	0.5 M H ₂ SO ₄	0.01 M	91.76	[75]
bis(p-(N,N,N-decyldimethylammonium bromide)benzylidene thiourea	carbon steel	1.0 M HCl	5.0 mM	94.09	[76]
N-(3-(Dimethyl benzyl ammonio)propyl) alkanamide chloride derivatives	mild steel	1.0 M HCl	0.5 mM	78.3- 93.1	[77]
Isoxazolium cationic Schiff bases	carbon steel	0.5 M HCl	0.66 – 0.81mM	88 - 91	[36]
WA-1	carbon steel	0.5 M HCl	100 ppm	98.25	Present work
WA-2	carbon steel	0.5 M HCl	100 ppm	97.29	Present work
WA-3	carbon steel	0.5 M HCl	100 ppm	93.10	Present work

LIST OF FIGURES

No.	Caption
Figure 1	Scheme 1. Synthetic route for the syntheses of the surfactants (WA-1 , WA-2 , WA-3)
Figure 2	Plotting of (A) surface tension and (B) specific conductivity against concentration of the synthesized cationic surfactants in water at 25 °C
Figure 3	Potentiodynamic polarization curves of carbon steel in presence of different concentrations of (A) WA-1 , (B) WA-2 and (C) WA-3 at 50 °C in 0.5 M HCl
Figure 4	Nyquist plots for carbon steel in 0.5 M HCl in the absence and presence of (A) WA-1 , (B) WA-2 and (C) WA-3 at 50 °C. (D) Equivalent circuit used to fit the EIS data
Figure 5	Langmuir adsorption isotherms for (A) WA-1 , (B) WA-2 and (C) WA-3 on carbon steel in 0.5 M HCl (surface coverage data were taken from the Potentiodynamic polarization data)
Figure 6	Optimized structures, HOMO, LUMO and MEP of the WA-2 and WA-1 inhibitor.
Figure 7	Side and top view of WA-2 and WA-1 inhibitor over Fe (110)

Figure 1

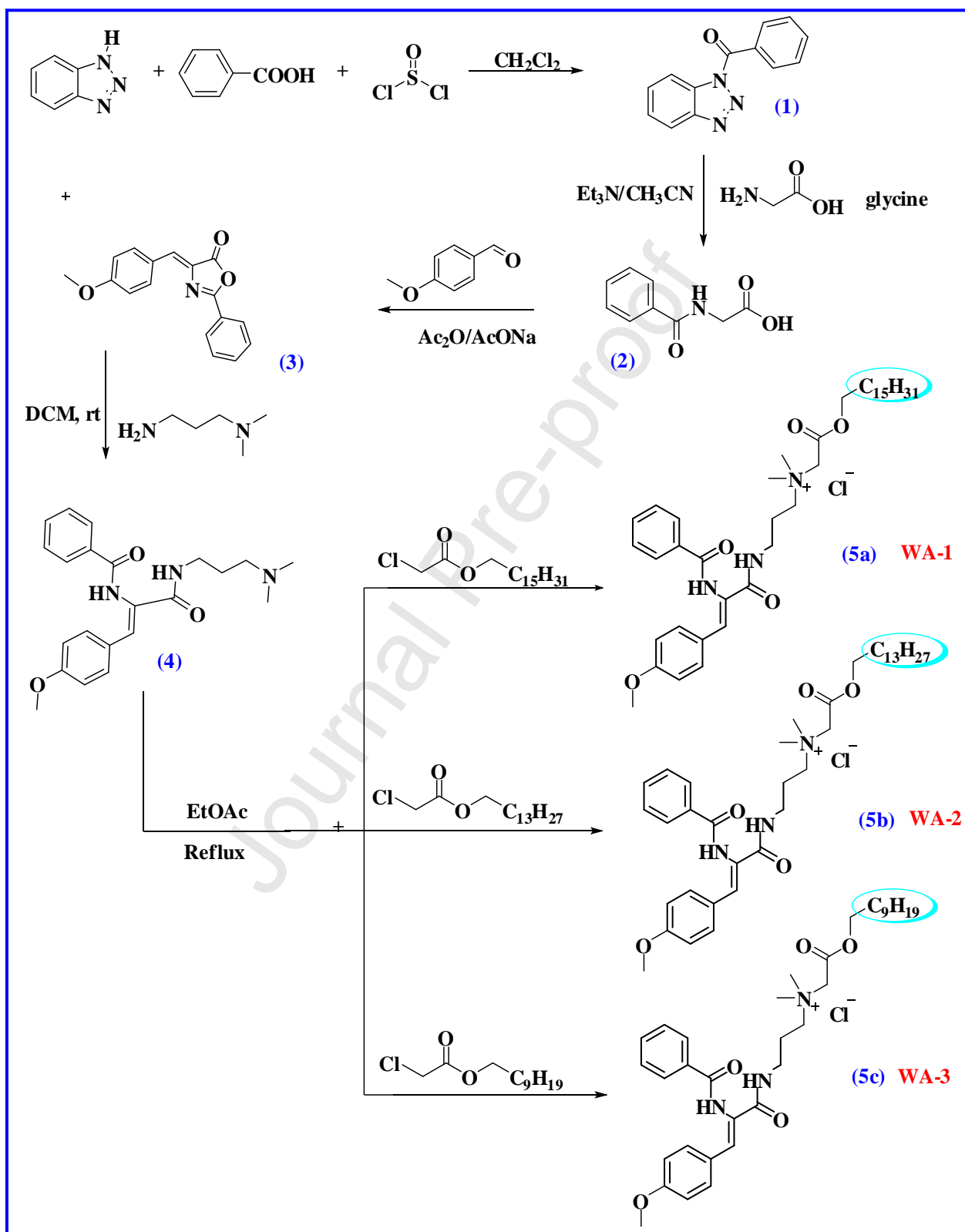


Figure 2

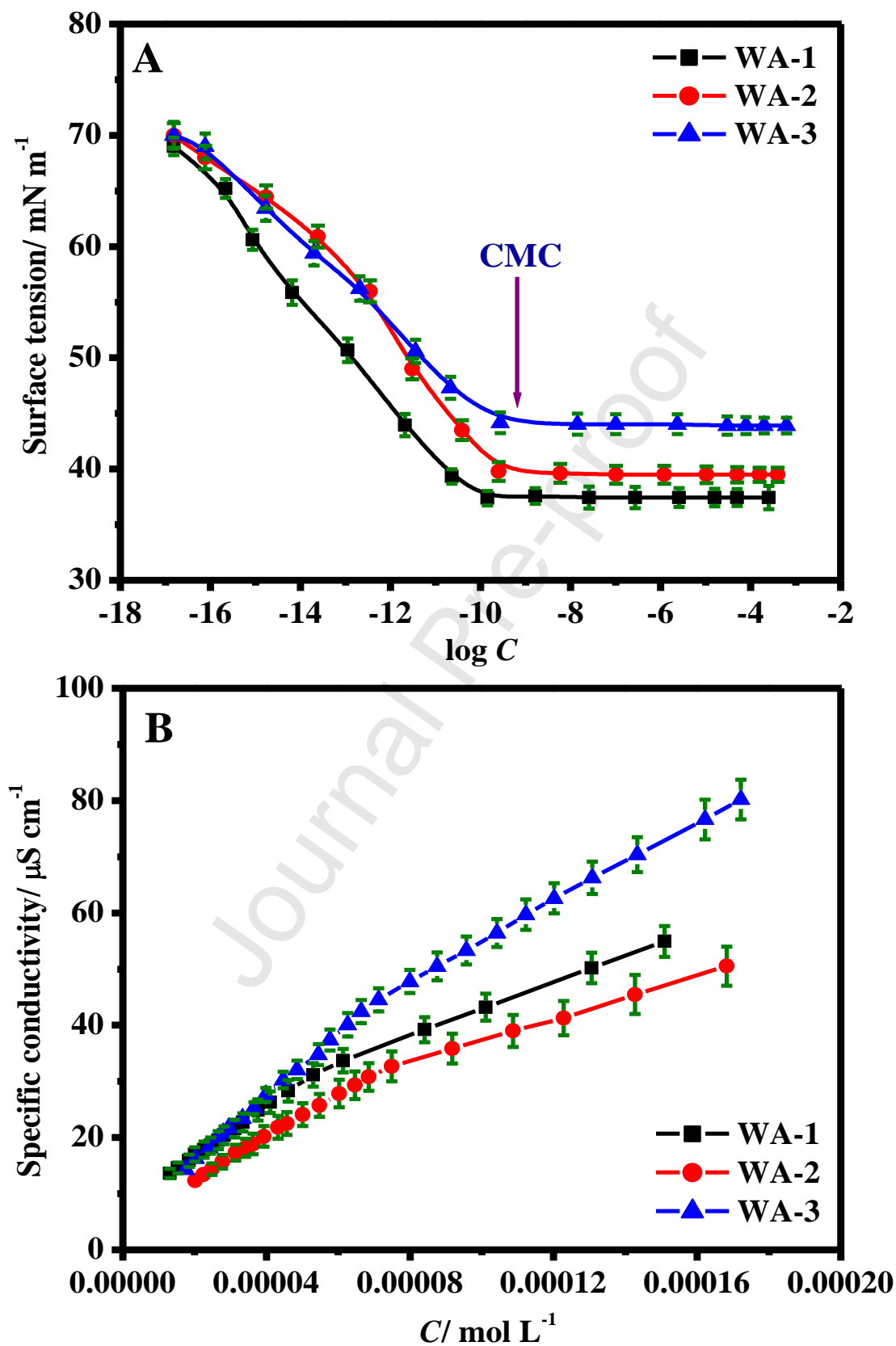


Figure 3

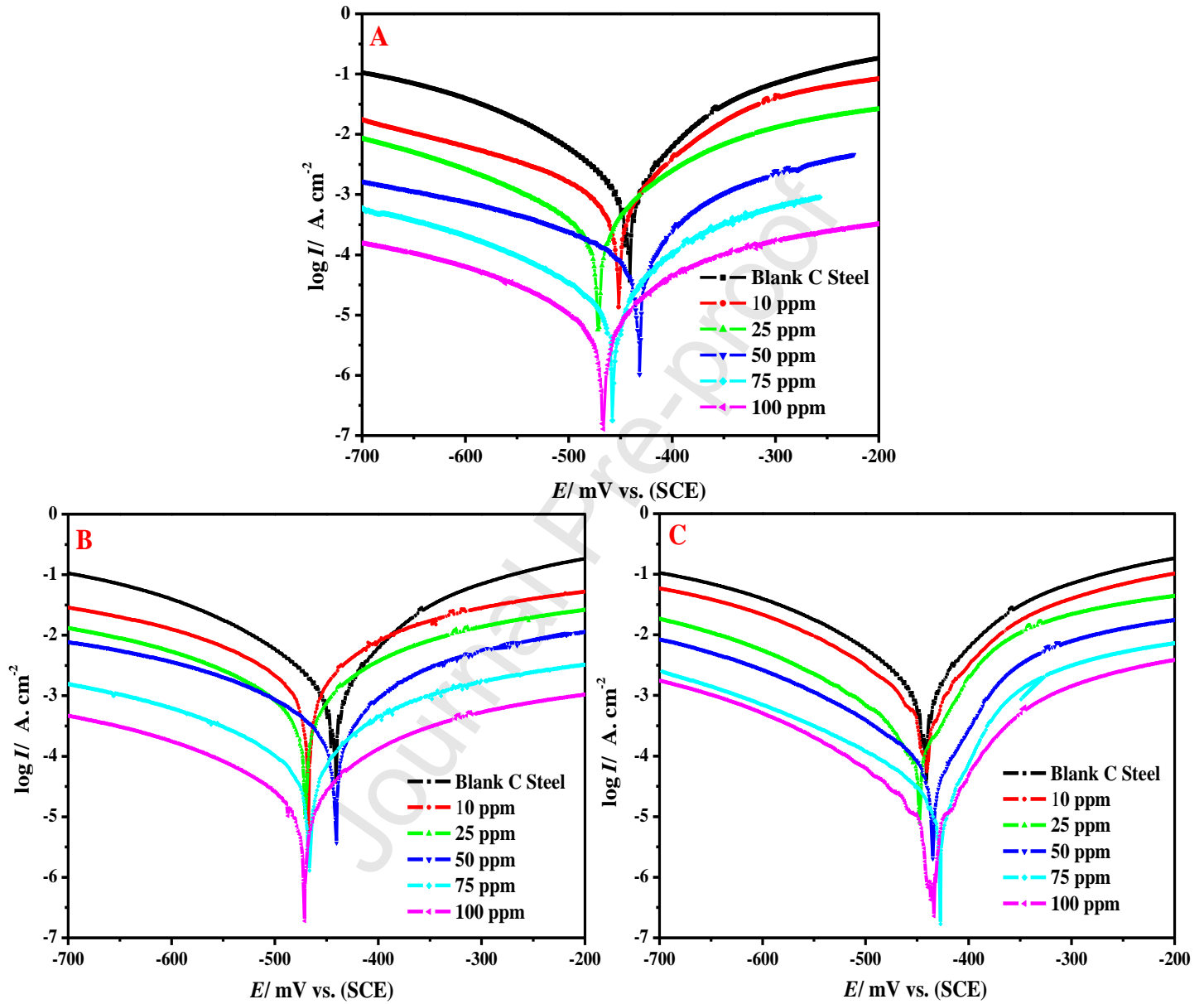


Figure 4

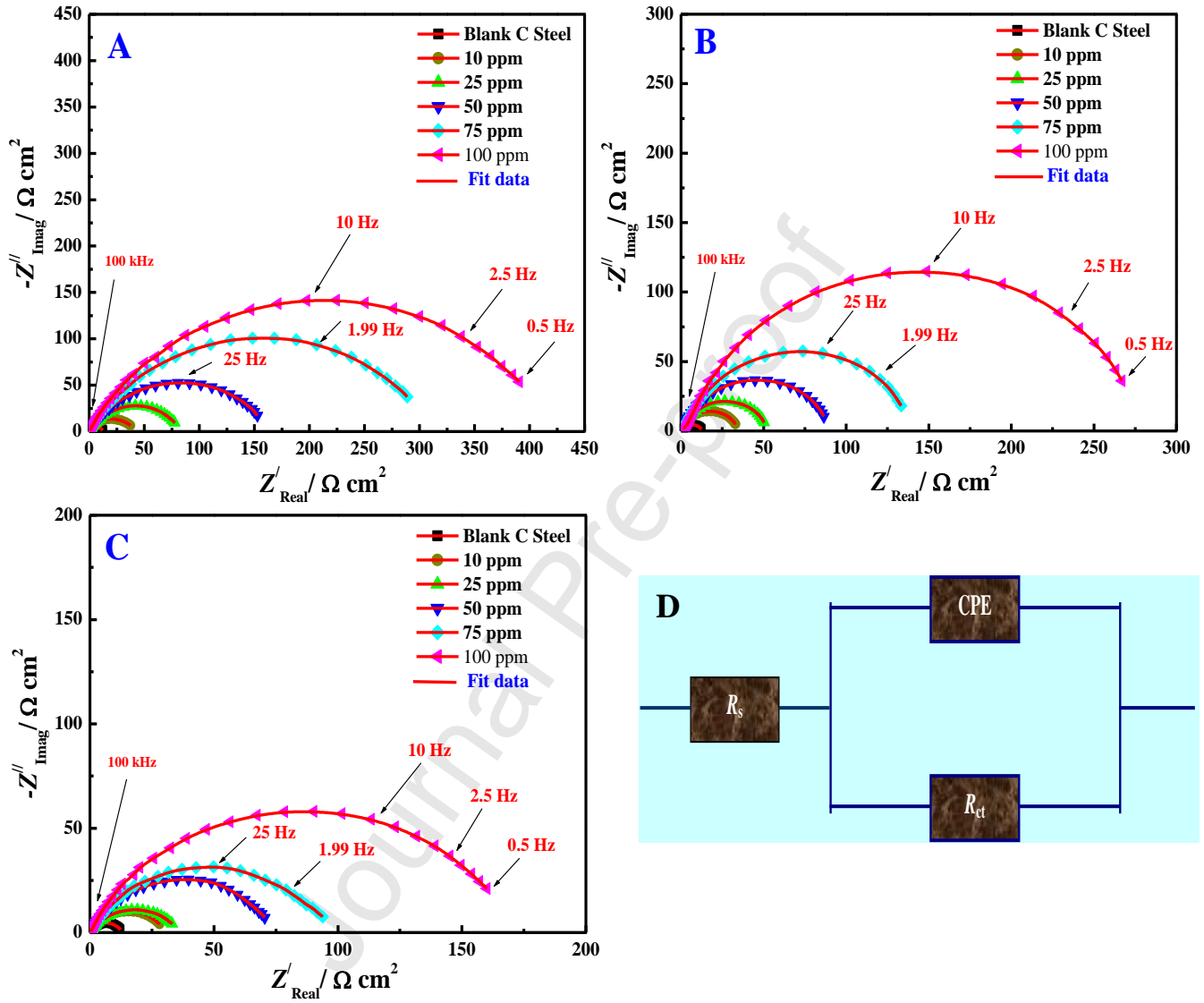


Figure 5

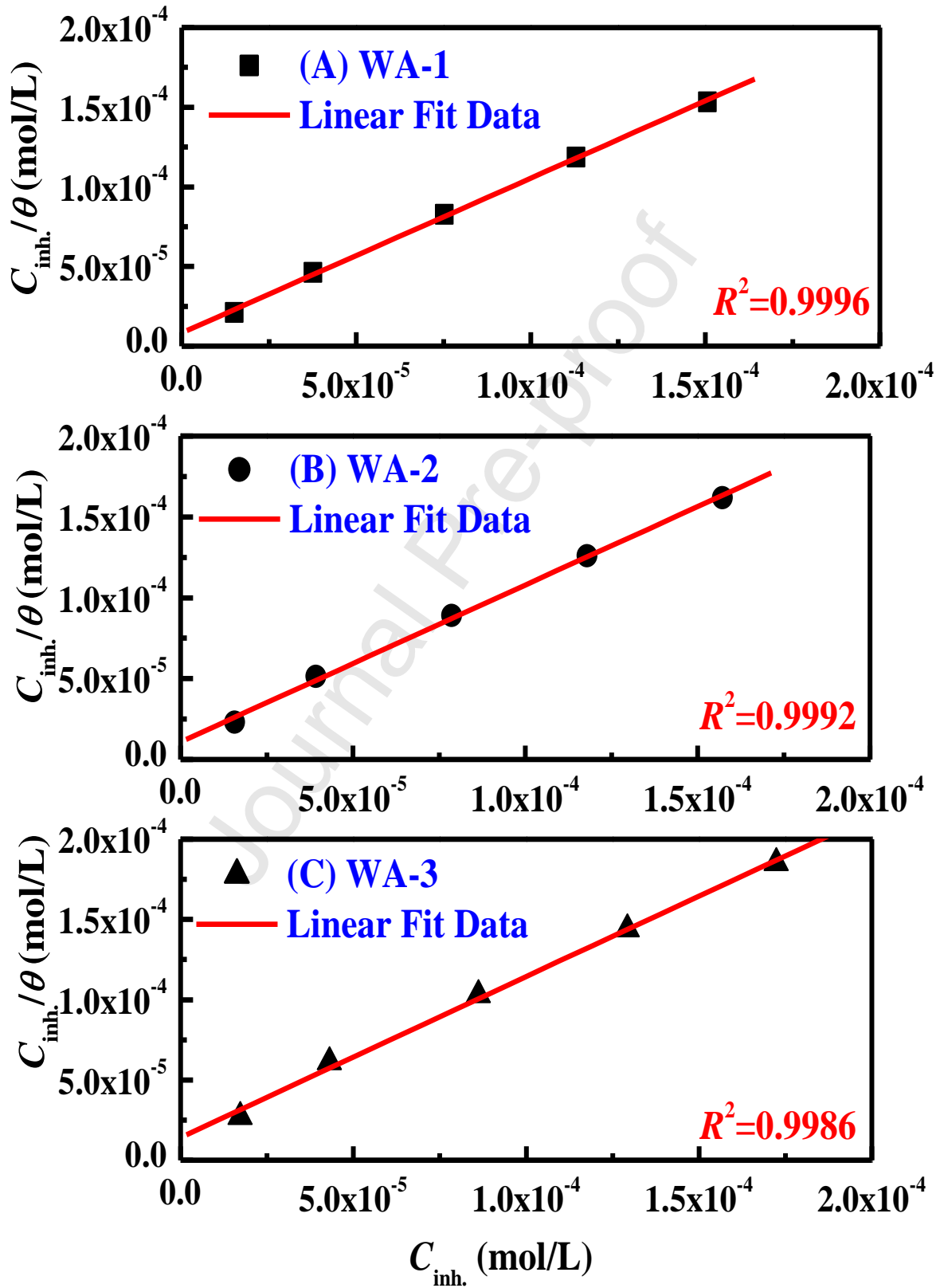
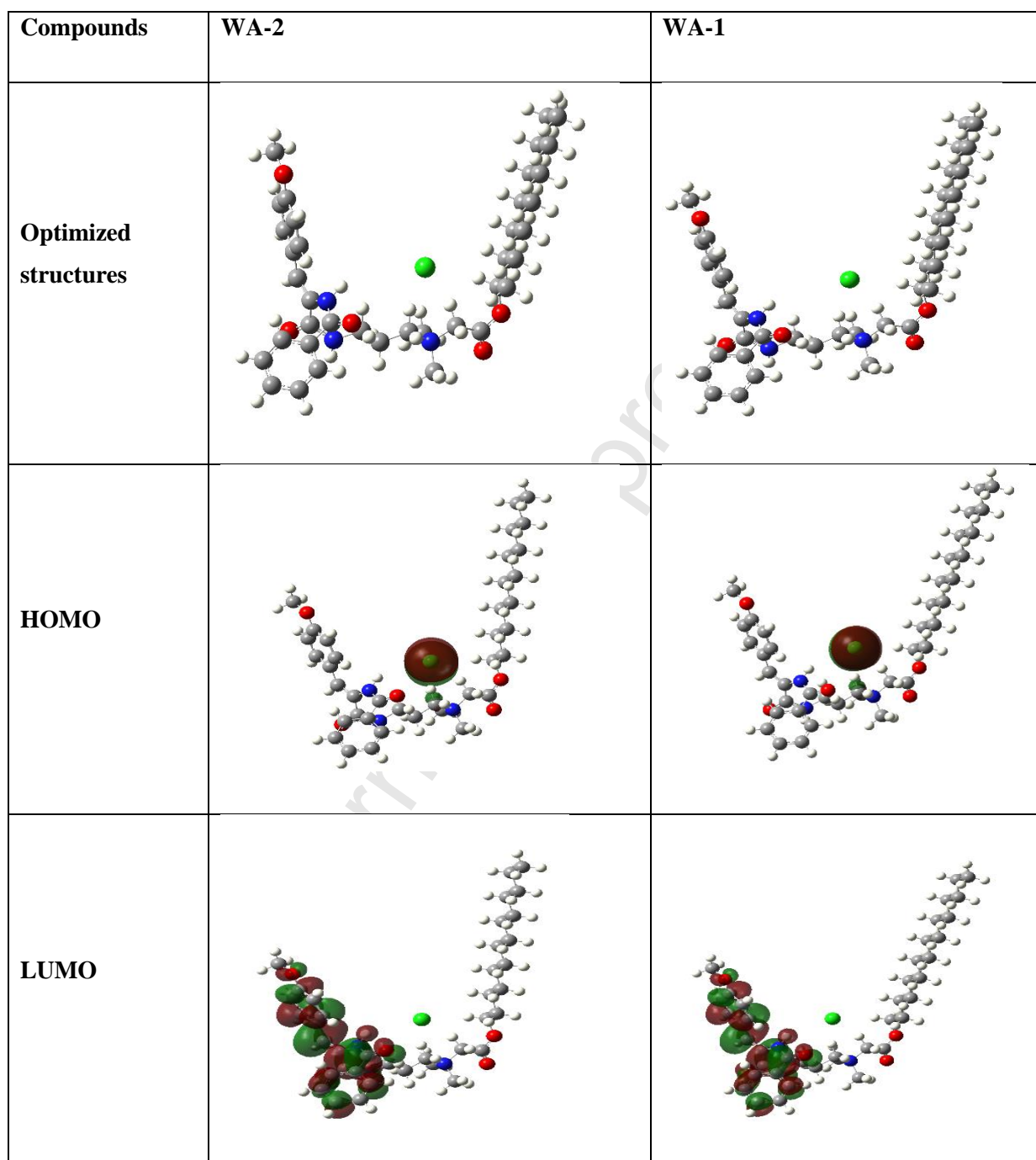


Figure 6

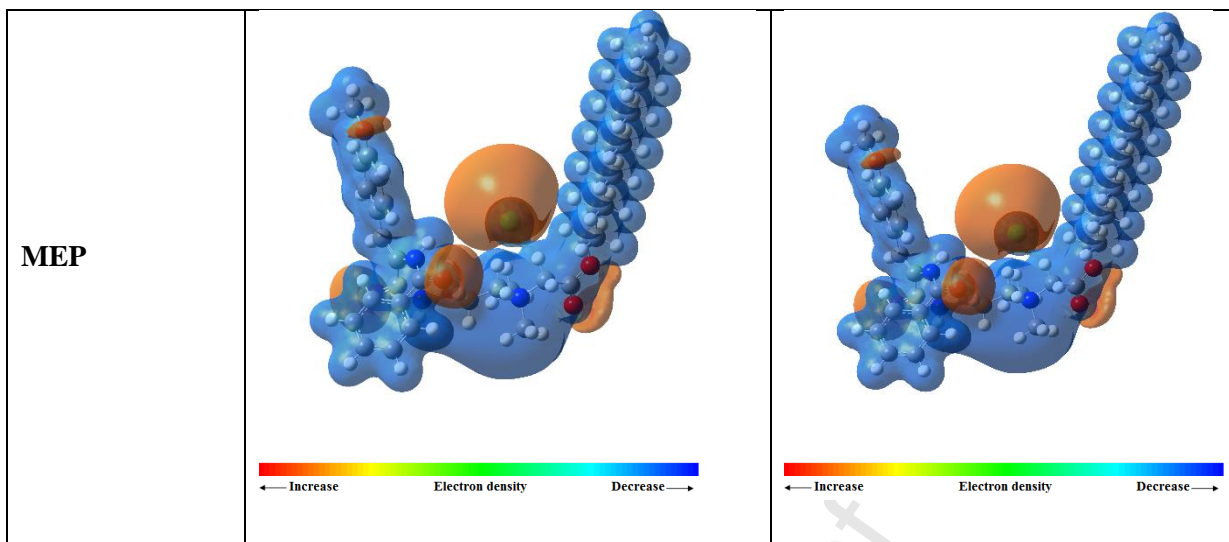
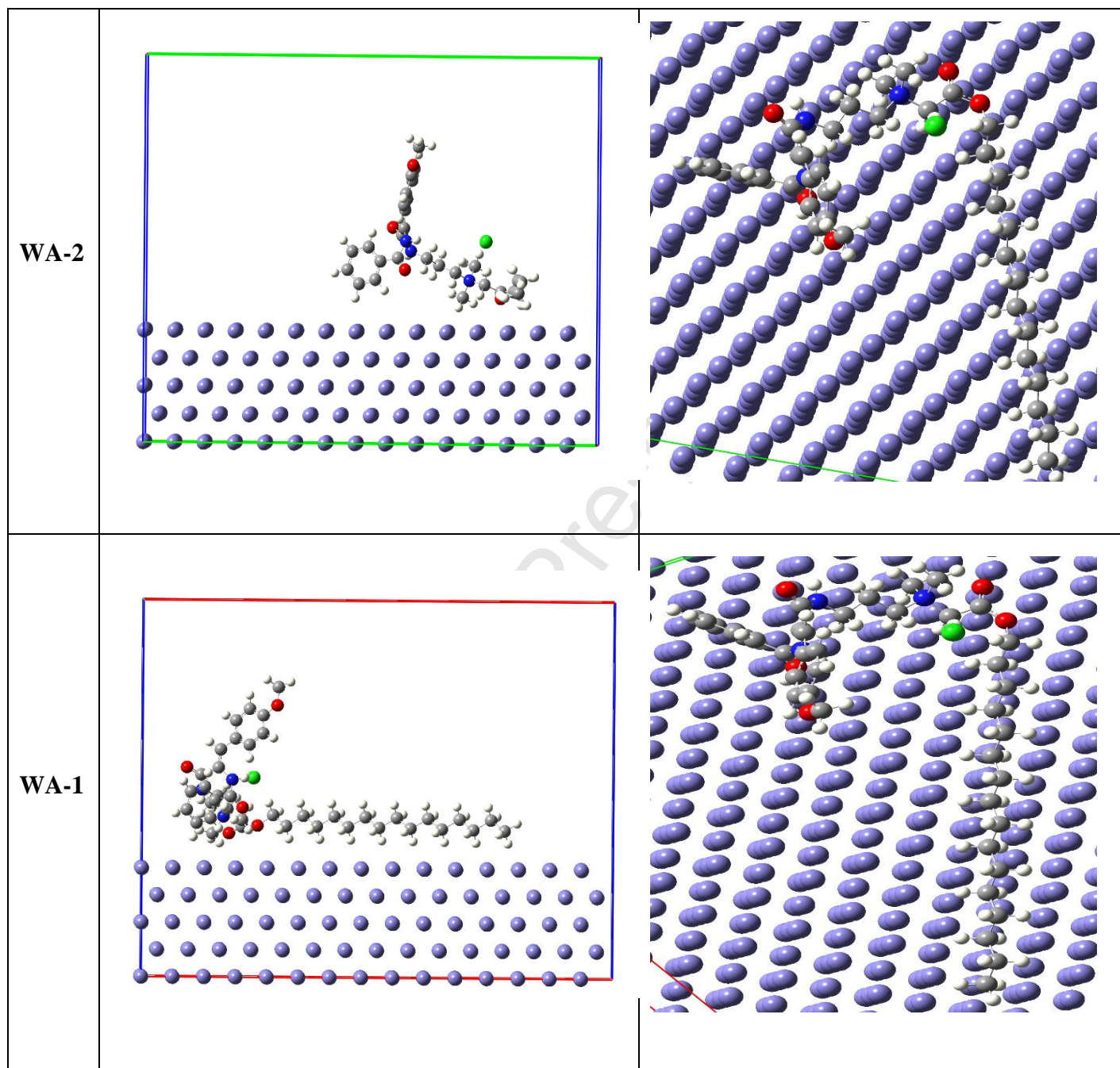


Figure 7**Declaration of interests**

■ The authors declare that they have no known competing financial interests or personal relationships that could have appeared to influence the work reported in this paper.

The authors declare the following financial interests/personal relationships which may be considered as potential competing interests:

Sincerely

Dr. Ahmed H. Tantawy

Journal Pre-proof

AUTHORSHIP STATEMENT

Manuscript title: Synthesis, assessment and corrosion protection investigations of some novel peptidomimetic cationic surfactants: empirical and theoretical insights

All authors certify that they have participated sufficiently in the work to take public responsibility for the content, including participation in the concept, design, analysis, writing, or revision of the manuscript. Furthermore, each author certifies that the content of this manuscript has not been published in a refereed journal, and it is not being submitted for publication elsewhere.

Authorship contributions

A.H. Tantawy, H. M. Abd El-Lateef and W. S. Abdrabo designed the research and implemented the experiments. B. Elgendy and K. A. Soliman designed the theoretical study. All authors analyzed data and wrote the manuscript. All the authors reviewed and validated the present manuscript prior to its being submitted.

Highlights

- Three novel Peptidomimetic Cationic Surfactants were synthesized based on acrylamide derivatives
- The inhibition and adsorption performance of these compounds on C-steel corrosion were investigated
- PDP studies demonstrated that the titled surfactants behaved as mixed-type inhibitors
- The adsorption of compounds on the electrode surface follows the Langmuir model
- MD simulations and DFT designs were accomplished to confirm experimental results